# Long Range Passive Ocean Acoustic Waveguide Remote Sensing (POAWRS) of Seismo-acoustic Airgun Signals Received on a Coherent Hydrophone Array

Sai Geetha Seri\*, Chenyang Zhu\*, Matthew Schinault\*, Heriberto Garcia\*, Nils Olav Handegard<sup>†</sup>, and Purnima Ratilal\*

\*Northeastern University, 360 Huntington Ave., Boston, MA 02115, USA

†Institute of Marine Research, Post Office Box 1870, Nordnes, N-5817 Bergen, Norway

Abstract-Airgun source systems generate low frequency underwater sound used in reflection and refraction seismology for mapping ocean bottom stratigraphy with important applications in ocean geosciences, such as understanding plate tectonics, ascertaining ocean geological history and climate change, and offshore hydrocarbon prospecting. Seismo-acoustic airgun signals from geophysical surveying activity were recorded at very long ranges, spanning roughly 175-195 km, on a large-aperture denselypopulated linear coherent hydrophone array in the Norwegian Sea during Spring 2014. Off the coast of Alesund, airgun signals were detected with 8 s inter-pulse intervals for 3 to 24 hour time periods per day over the 4 days of hydrophone array operation in that region. Here we provide a time-frequency characterization and bearing-time estimation of the received airgun pulses. By correcting for transmission losses in the rangeand depth-dependent Norwegian Sea environment, we estimate the source level distribution back projected to a distance of 1 m from the airgun source system. This back-projected source level distribution is then applied to model the Probability of Detection (PoD) region for the airgun signals with the coherent hydrophone array as the receiver in the Norwegian Sea employing the passive ocean acoustic waveguide remote sensing (POAWRS) technique. The estimates of back-projected source level distribution and PoD region provide an understanding of the horizontal spatial propagation extent of the signals from the airgun source system in the shallow and deep water regions of the Norwegian Sea. These results can also be applied to studies of the potential impact of airgun signals on marine organisms.

Index Terms—seismic airgun source, passive ocean acoustic waveguide remote sensing, source level

#### I. Introduction

Airgun source systems are employed as seismo-acoustic sources in reflection and refraction seismology for mapping ocean bottom stratigraphy with important and critical applications in ocean geosciences [1]–[8]. These include understanding ocean plate tectonics, developing geological models of the continental and ocean crust, ascertaining ocean geological history and climate change, as well as in offshore hydrocarbon prospecting. Seismic surveys are essential in hydrocarbon exploration to help reduce the risk of unnecessary drilling by predicting potential reservoir locations. To mitigate absorption losses in the sea bottom and ensure significant

bottom penetration depth of several kilometers, airgun source systems often generate intense seismo-acoustic signals. This is accomplished with an airgun array comprised of multiple airgun elements with specified inter-element spacing whose radiated signals can coherently combine to raise the overall sound pressure level, especially in the main beam of the airgun array, directed towards the sea bottom. Low frequency airgun signals can sometimes be found in underwater passive acoustic recordings of the ocean environment with single or multi-channel hydrophone monitoring systems [9]–[11]. When present, they are highly repetitive and can be a significant source of low frequency man-made sound. The intensity of the airgun signals have generated concerns leading to investigations of the potential impact or lack of on marine organisms [12]–[17].

Here we provide an analysis of repetitive airgun pulsed signals found in the recordings of a large-aperture denselysampled linear coherent hydrophone array system located at very long ranges, spanning 175 km to 195 km, from an airgun source in the Norwegian Sea. The coherent hydrophone receiver array data is processed using the passive ocean acoustic waveguide remote sensing (POAWRS) technique [18]-[22] to provide automatic detection, bearing-time estimation and timefrequency characterization of the received airgun pulses. We estimate the back-projected source level distribution of the received airgun signals, back projected [23] to a distance of 1 m from the airgun source system by correcting for transmission losses in the range- and depth-dependent Norwegian Sea environment. The back-projected source level distribution is then applied to calculate the Probability of Detection (PoD) region for the airgun signals in both the shallow and deep water regions of the Norwegian Sea.

As discussed in [23], the standard measure of a source array's strength is estimated by correcting the received pressure level measured in the far-field of the source with the transmission loss that corrects for geometrical spreading and absorption loss, back to a notional distance of 1 m from the source array's geometrical center. This resulting estimated back-projected source level is not achieved in reality because

the array elements are not adding coherently in the nearfield vicinity very close to the source array elements. Despite this, the back-projected source level is still a useful quantify for calculations and applications in the far-field.

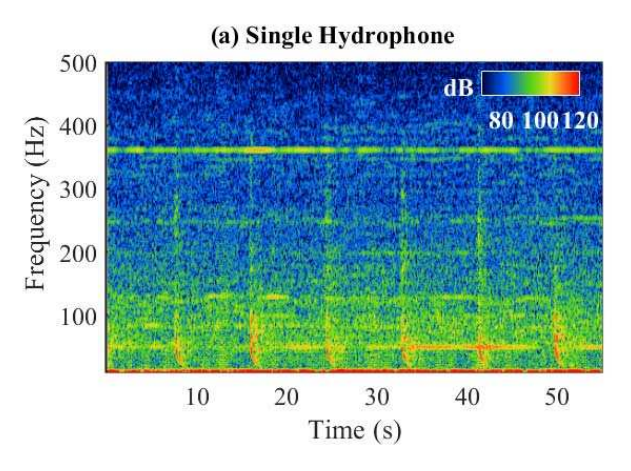
The POAWRS technique has been previously employed to detect and characterize various underwater sound sources received using a coherent hydrophone array, such as marine mammal vocalization signals from both baleen and toothed whale species [18], [19], [22], [24], [25], as well as sounds generated by ocean vessels [20], [21]. Off the coast of Norway, in both the Norwegian and Barents Seas, the POAWRS technique has been applied to examine vocalization types, as well as quantify call rates and spatial distributions of fin whale vocalizations [19] recorded in the same data set as that analyzed here. The POAWRS technique has also been applied to detect, characterize and localize multiple surface ships over instantaneous wide areas of the Norwegian and Barents Seas, spanning 100 km or more in diameter, from their sounds radiated underwater [20], [21].

Passive acoustic methods have been used in the past to examine, characterize and estimate the back-projected source level and sound exposure levels of airgun signals [23], [26]. Propagation of airgun signals in the shallow continental-shelf region (≤ 200 m depth) of the Norwegian Sea has been modelled using ray tracing and verified with experimental data acquired using standalone hydrophones located at a maximum distance of 30 km from the source [10], applied to assess the potential impact of airgun signals on fish populations.

# II. MATERIAL AND METHODS

The seismo-acoustic airgun signals analyzed here were recorded during the Norwegian Sea 2014 Experiment (NorEx14), conducted by a collaborative team from the Massachusetts Institute of Technology, Northeastern University, NOAA-Northeast Fisheries Science Center, Naval Research Laboratory, Penn State University, and the Woods Hole Oceanographic Institution in the United States, as well as the Institute of Marine Research-Bergen (IMR) in Norway. The NorEx14 was conducted from 18 February to 8 March 2014, in conjunction with the IMR survey of spawning populations of Atlantic herring off the Alesund coast, the Atlantic cod off the Lofoten peninsula [27], and the capelin off the Northern Finnmark region. Airgun signals were present in underwater acoustic recordings off the Alesund region from 18 February to 21 February 2014, but absent in recordings off the Lofoten peninsula and the Northern Finnmark region for the remaining duration of the experiment.

In NorEx14, recordings of underwater sound were acquired using a horizontal linear coherent hydrophone array towed at an average speed of 4 knots (roughly 2 m/s) along designated tracks for 8-24 hours per day. To minimize the effect of tow ship noise on the recorded acoustic data, the coherent hydrophone array was towed approximately 280-330 m behind the research vessel so as to confine this noise to the forward endfire direction of the array, which is the forward direction parallel to the array axis. The tow ship noise in directions



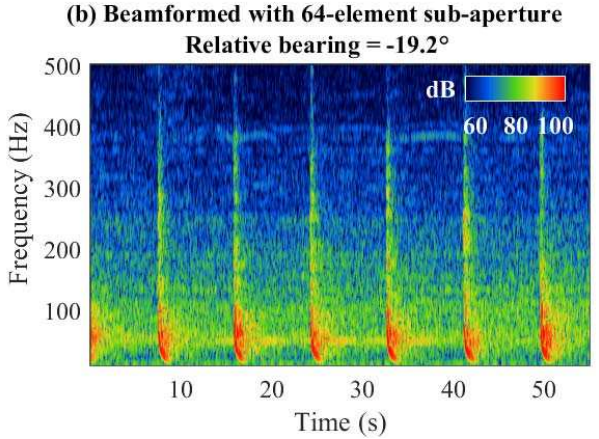


Fig. 1: Coherent array processing enhances the SNR to aid in the detection of repetitive seismo-acoustic airgun signals. Compare single hydrophone measured spectrogram in (a) with spectrogram after coherent beamforming in (b) with 64-element ULF sub-aperture of POAWRS 160-element hydrophone array.

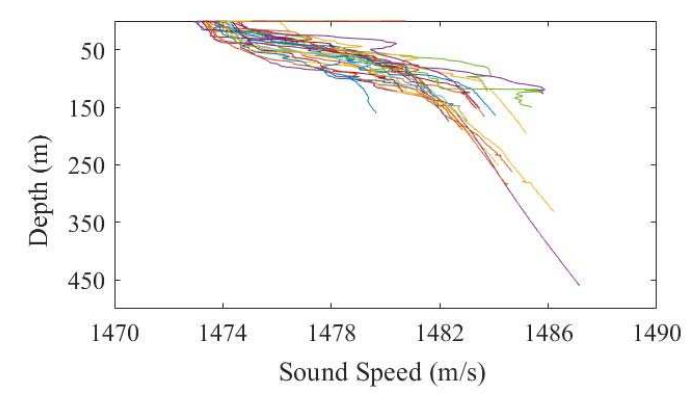


Fig. 2: Water-column sound speed profiles derived from XBT measurements in the shallow water region off Alesund coast in the Norwegian Sea.

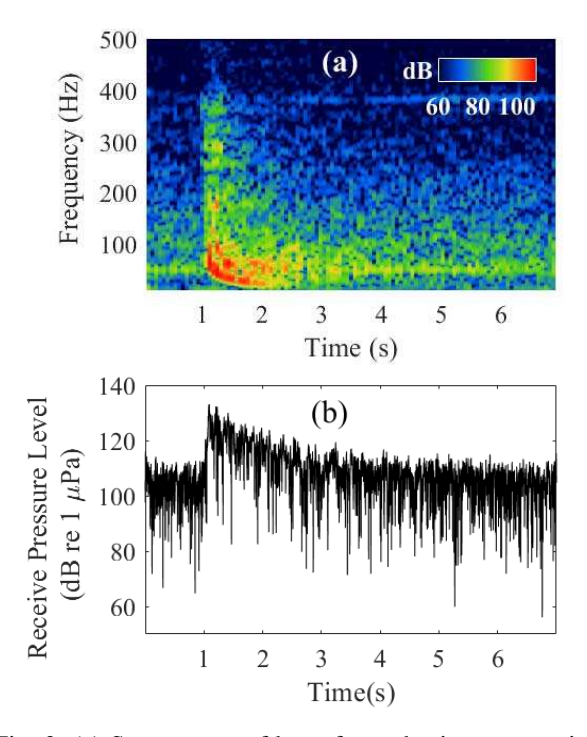


Fig. 3: (a) Spectogram of beamformed seismo-acoustic airgun signal received on the coherent hydrophone array. (b) Received pressure level of the corresponding airgun signal.

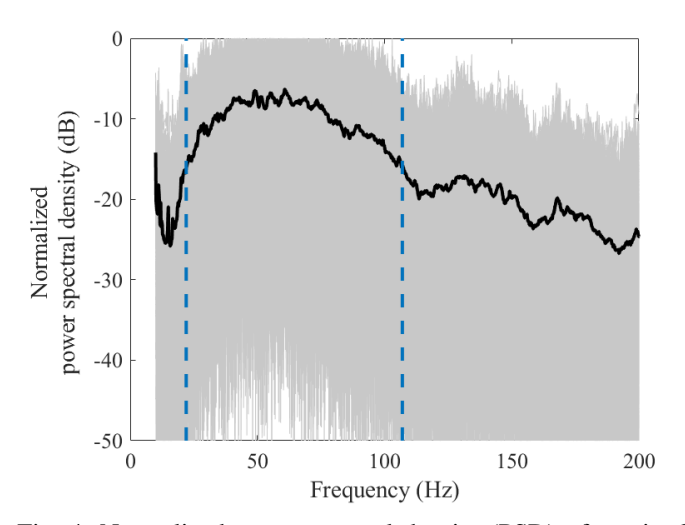


Fig. 4: Normalized power spectral density (PSD) of received airgun signals. The gray curves shows the PSD of 1482 signal detections. The black curve is the mean PSD and the blue dotted lines bound the -10 dB bandwidth with  $f_L=22~{\rm Hz}$  and  $f_U=107~{\rm Hz}$  respectively.

away from the forward endfire was negligible after coherent beamforming. The water depth ranged from 100 to 300 m at the array locations, and the array tow depth varied from 45 to 70 m in NorEx14.

The coherent hydrophone array is composed of multiple nested sub-apertures with 160 hydrophones in total, spanning

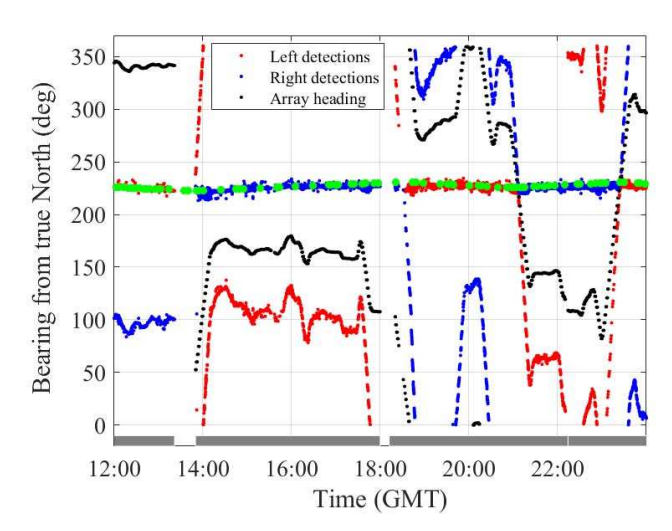


Fig. 5: Bearings of received airgun signals from true North and array heading measured on 18 February, 2014, in the Alesund region. The green dots are the calculated bearings of the ocean vessel, MV Vestland Mistral, that match well with the true bearings of airgun signal detections. The light gray bar at the bottom show the coherent hydrophone array recording time intervals.

a frequency range from below 15 Hz to 4 kHz for spatially unaliased sensing. The mean sensitivity of each hydrophone is a constant in this frequency range. A fixed sampling frequency of 8000 Hz was used so that acoustic signals with frequency contents up to 4000 Hz were recorded without temporal aliasing. Two linear nested sub-apertures of the array, the ultra low-frequency (ULF) and low-frequency (LF) sub-apertures, each consisting of 64 equally spaced hydrophones with interelement spacings of 3 m and 1.5 m respectively, were used to analyze the seismo-acoustic airgun signals with dominant frequencies below 500 Hz.

The detection of long-range propagated sounds is significantly enhanced by spatial beamforming and spectrogram analysis which filters the background noise that is outside of the beam and frequency band of the airgun signals. The high gain of the coherent 64-hydrophone sub-apertures, of up to  $10\log_{10}64=18$  dB, enabled detection of the airgun signals with higher signal-to-noise ratio (SNR) than a single omnidirectional hydrophone, which has no array gain as in Figure 1. The actual array gain, which may be smaller than the full 18-dB theoretical array gain, is dependent on noise coherence and signal wavelength relative to array aperture length. For example, the array gain for the airgun signals recorded here near peak frequency of 60 Hz is 8.9 dB.

Physical oceanography was monitored by sampling water-column temperature and salinity with expendable bathy ther-mographs (XBTs) and conductivity-temperature-depth (CTD) sensors at regular intervals of a couple of hours each day. The water-column sound speed profile measured in the continental-shelf region off Alesund, is shown in Figure 2. The sound

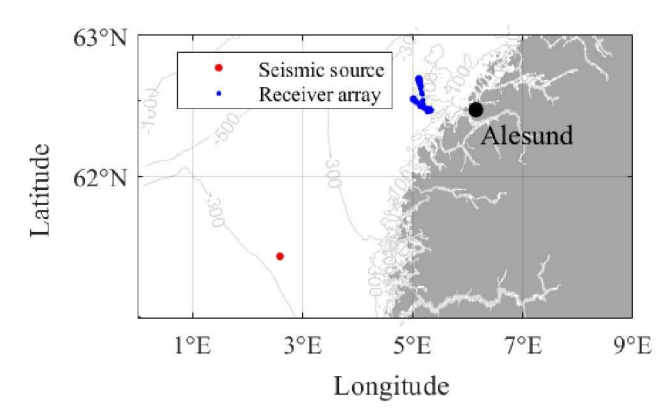


Fig. 6: Track of ocean vessel carrying airgun source system (in red) and locations of the coherent hydrophone receiver array (in blue) on 18 February, 2014.

speed profile for water depths deeper than roughly 250 m in the Norwegian Sea, required for transmission loss modeling, is interpolated according to Figure 4(b) of [28] and Figure 10 of [29].

Airgun signal detection, bearing estimation and temporalspectral characterization

Seismo-acoustic pressure time series measured by sensors across the receiver array were converted to two-dimensional beam-time series by beamforming [30]. A total of 64 beams were formed spanning 360 degree horizontal azimuth about the receiver array for data from the ULF sub-aperture. Each beam-time series was converted to a beamformed spectrogram by short-time Fourier transform (sampling frequency = 8000 Hz, frame = 2048 samples, overlap = 3/4, Hann window). Significant sounds present in the beamformed spectrograms were automatically detected by first applying a pixel intensity threshold detector [19], [20], [31] followed by pixel clustering, and verified by visual inspection. The horizontal azimuthal direction or bearing of each detected signal, measured from array broadside, is estimated by coherent beamforming that selects the bearing in which the beamformed, band-pass filtered pressure-time series contained maximum energy during the time duration of the signal and in the same frequency band. The estimated relative bearings, measured with respect to array broadside are then converted to absolute bearings, measured from the array centre with respect to true North.

The airgun signal detections are automatically grouped by cluster analysis of the time-frequency features extracted from pitch-tracking of the signal detections. The pitch-tracking and cluster analysis of POAWRS data is described in [19]–[21]. The extracted airgun signal detection clusters are verified by visual inspection of their pitch tracks and randomly selected spectrograms. The airgun source system location is next found by identifying the seismic survey vessel that deployed the airgun source system. The true bearing-time trajectory of received airgun signal detections are overlain with true bearings of known ocean vessels in the Alesund region, calculated

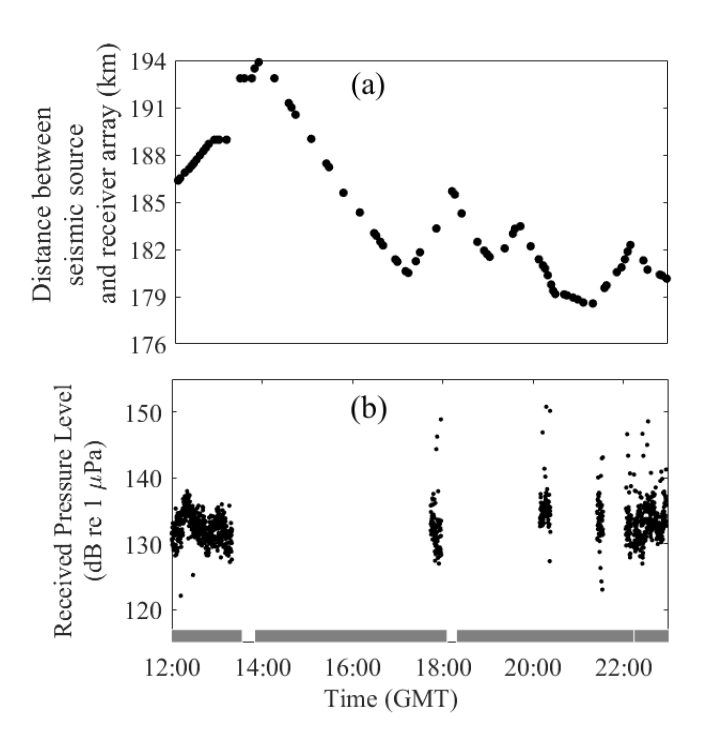


Fig. 7: The horizontal separation distance between airgun source system and coherent hydrophone receiver array in the Alesund region on 18 February 2014, is shown in (a). Calculated received pressure level of 1482 seismo-acoustic airgun signal detections measured by the coherent hydrophone array on that day is shown in (b). The light gray bar at the bottom shows the coherent hydrophone array recording time intervals.

from the global positioning system (GPS) locations of each vessel and the hydrophone array. The seismic survey vessel is identified by matching the bearing-time trajectory of the detected airgun signals with those of known surface ships.

Back-projected source level estimation and Probability of Detection (PoD) region modeling for the airgun signals

The back-projected source level  $SL(r_0)$  of each seismic airgun signal is estimated from its received pressure level RL(r) via the passive sonar equation [19], [32], [33],

$$SL(\mathbf{r_0}) = RL(\mathbf{r}) + TL(|\mathbf{r} - \mathbf{r_0}|). \tag{1}$$

where  $\mathbf{r}$  is the location of the coherent hydrophone array center and  $\mathbf{r}_0$  is the location of the airgun source system.

The received pressure level (RPL) of the airgun pulse is estimated as the RMS value of the maximum instantaneous time-domain signal bandpass-filtered between upper  $f_U$  and lower  $f_L$  frequencies and beamformed to the azimuthal bearing of the received airgun signal, over a time window encompassing over 90% of the total signal energy. The upper  $f_U$  and lower  $f_L$  frequencies are determined as the -10 dB end points relative to the signal peak in the power spectrum.

The corresponding one-way broadband acoustic transmission loss,  $TL(|\mathbf{r}-\mathbf{r_0}|)$ , from the location of the airgun

source system to the centre of the POAWRS receiver array, was calculated using a calibrated parabolic equation-based range-dependent acoustic propagation model (RAM) [19], [34], [35] via,

$$\mathrm{TL}(|\mathbf{r}-\mathbf{r_0}|) = 10 \log_{10} \big( \int_{f_L}^{f_U} Q(f) \langle |G(\mathbf{r}|\mathbf{r_0},f)|^2 \rangle df \big), \ (2)$$

where  $G(\mathbf{r}|\mathbf{r_0},f)$  is the waveguide Green function at frequency f for the airgun source located at  $\mathbf{r_0}$  and receiver at  $\mathbf{r}$ , Q(f) is the normalized airgun signal spectra, and  $f_U$  and  $f_L$  are the upper and lower frequencies used for the bandpass filter. The airgun source depth and the receiver array depth used in the calculations are 25 m and 50 m respectively.

The model takes into account the environmental parameters, such as the range-dependent water depth and sound speed profiles (Figure 9(b)) measured in the Norwegian Sea to stochastically compute the propagated acoustic intensities via Monte-Carlo simulations following the approach of [36]–[38]. Internal waves are simulated by updating the sound speed profiles in range every 200 m. Since it is not possible to predict the exact characteristics of internal wave such as direction, amplitude and frequency, the profiles are selected randomly from the recording during the experiment. The water depth in the region varied drastically, from less than 100 m in shallow waters approaching shore-wards of Alesund to over 3000 m in deep waters off the continental slope, significantly impacting the propagation of the seismo-acoustic signals (Figure 9(d)-(f))

The POAWRS PoD region for the seismo-acoustic airgun signals in the Norwegian Sea, as a function of range from the coherent hydrophone receiver array is calculated following the formulation provided in Appendix A of [19], [20].

### III. RESULTS AND DISCUSSIONS

Here, results from analysis of the seismo-acoustic airgun signal detections in the 10 to 200 Hz frequency range measured by the coherent hydrophone array off the Alesund region in the Norwegian Sea on 18 February 2014 are presented and discussed. An example spectrogram containing repetitive airgun pulsed signal detections is shown in Figure 1. Even though the spectogram in Figure 1 indicates the airgun signals have a broad spectra ranging from 10 Hz to 500 Hz, we find most of the energy concentrated in the 10-200 Hz frequency range. As shown in Figure 4, the -10 dB bandwidth for the power spectral density is 85 Hz wide, bounded by 22 Hz and 107 Hz. We analyze a subset of 1482 airgun signal detections received on the coherent hydrophone array on 18 February 2014 that is devoid of overlapping signals from other sound sources, such as marine mammal vocalizations and broadband ship-radiated underwater sound measured during the experiment. The bearing and time of beamformed airgun signal detections in the 10-200 Hz frequency range that stand at least 5.6 dB above the local ambient background noise are shown in Figure 5. When the bearing of the known ocean vessels in the Alesund region for that day are overlain, it

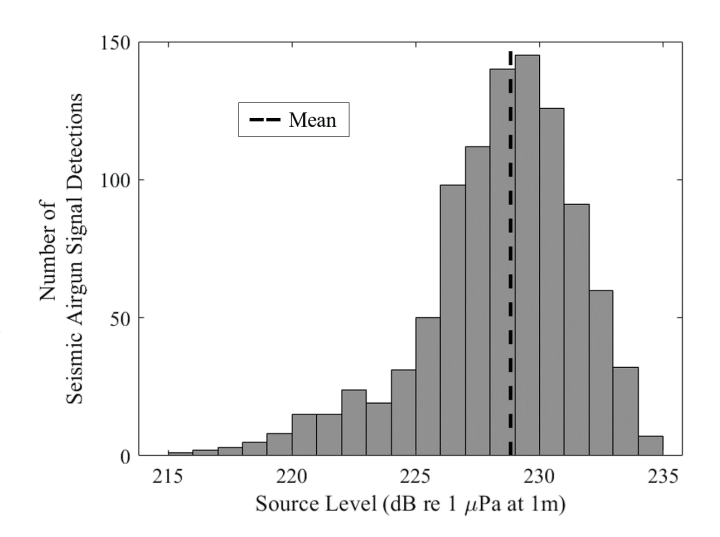


Fig. 8: Histogram of back-projected source level estimates of 1482 seismo-acoustic airgun signal detections off the Alesund region in NorEx14. The estimated back-projected source levels range from 210 to 235 dB re 1  $\mu$ Pa at 1 m with mean and standard deviation of 228.8  $\pm$  3.2 dB re 1  $\mu$ Pa at 1 m.

was found that the bearing-time trajectory of the vessel MV Vestland Mistral coincides well with the true bearing-time trajectory of the airgun signal detections. Figure 6 shows the location and track of the MV Vestland Mistral that deployed the airgun source, as well as the locations and track of the coherent hydrophone array deployed from a separate research vessel during the experiment. It was found that the horizontal distance of the airgun source system from the receiver array varied between 175-195 km as shown in Figure 7(a).

The received pressure level (RPL) of the majority of airgun signal detections are found to range from roughly 125 dB re 1  $\mu$ Pa to 140 dB re 1  $\mu$ Pa, as shown in Figure 7(b). The corresponding back-projected source level distribution derived from the received pressure levels of the airgun signals detections after correcting for transmission losses in the Norwegian Sea environment are shown in Figure 8. The estimated back-projected source levels of the airgun signals range from 210 to 235 re 1  $\mu$ Pa at 1 m. The mean and the standard deviation of the estimated source level distribution is 228.8  $\pm$  3.2 dB re  $\mu$ Pa at 1 m. The transmission losses in three distinct azimuthal directions as a function of range and water depth are plotted Figure 9(c-f). The modeled transmission losses are strongly dependent on bathymetry.

The estimated back-projected source level distribution for the airgun signals are next applied to calculate the PoD region for both the coherent hydrophone array as a receiver and for a single hydrophone as a receiver. The 50% PoD region, plotted in Figure 9(a), with the 64-element ULF sub-aperture of the coherent hydrophone array as the receiver, extends over an area more than 500 km in diameter depending on bathymetry and azimuthal direction. In contrast the single omnidirectional hydrophone provides no array gain and so the 50% PoD

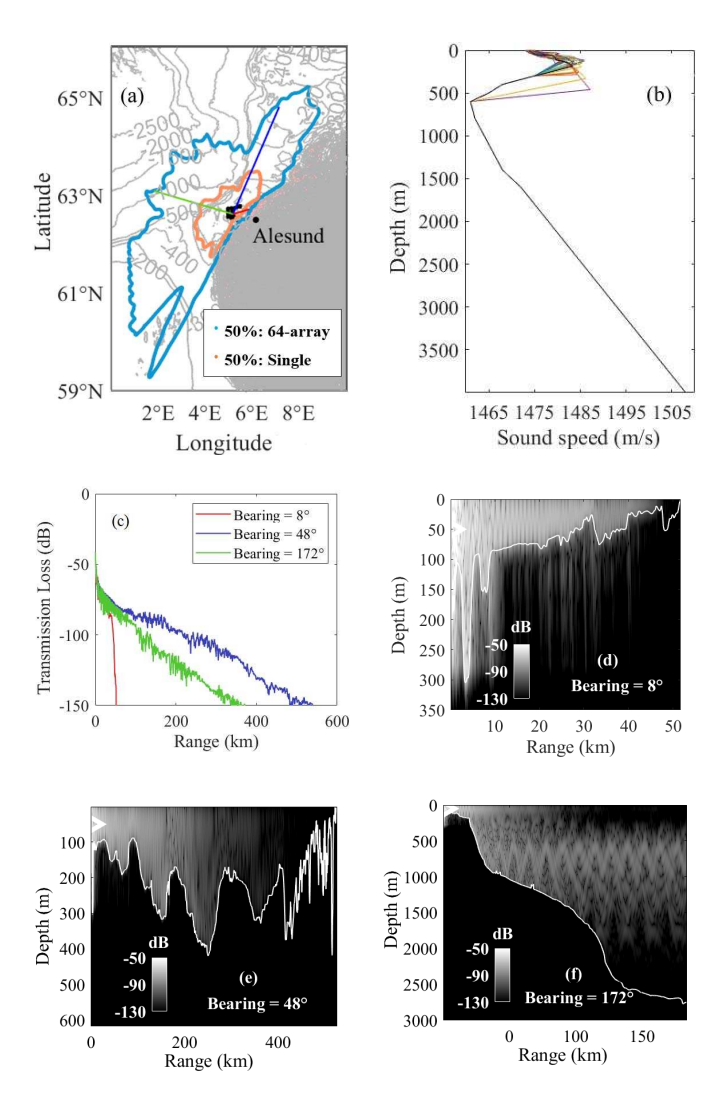


Fig. 9: The PoD region for seismo-acoustic airgun signal detections centered at 60 Hz, off the Alesund coast is shown in (a). The tow tracks of the coherent hydrophone array during 18 February 2014 are indicated in solid black. The solid contours provide the 50% PoD region for airgun signals received on the 64-element subaperture of the coherent hydrophone array after beamforming (in cyan) and the 50% PoD region for airgun signals received on a single hydrophone (in orange). Solid colored lines show three propagation paths with the following directions: 8°, 48°, and 172°. The sound speed profiles used in the acoustic propagation model are shown in (b). Transmission losses, as a function of range, calculated by a calibrated parabolic equation-based RAM model are shown in (c). The modeled broadband waveguide Green functions averaged over 15 Monte Carlo simulations along the three propagation paths are shown in (d)-(f) respectively.

region is significantly smaller. The detection range of the airgun signals is decreased in shoreward directions due to significant penetration and absorption in the sea bottom. The detection range extends roughly 200 km from the coherent

hydrophone array for airgun source systems in azimuthal directions pointing away from the shore and towards deep water.

According to [11], [26], the source level of a single airgun, which depends on the air volume, is assumed to range between 216-232 dB re  $\mu$ Pa at 1 m, while a full array of airguns generally used in seismic surveys is assumed to produce source level of up to 258 dB re  $\mu$ Pa at 1 m [23], [26]. Here, the back-projected source level is found to be 228.8  $\pm$  3.2 dB re  $\mu$ Pa at 1 m, which is roughly two orders of magnitude less intense than that assumed for a full airgun source array, and closer to the intensity assumed for a single airgun. The airgun system back-projected source level estimates obtained here are based on long range observations, 175-195 km range, and therefore dependent on the transmission loss correction. Measurements over a larger range span from close vicinity to several hundred kilometer separation between airgun source system and coherent hydrophone array, as well as larger sample sizes would be necessary to gain a better understanding of the effect of the environment on the propagation of these low frequency seismo-acoustic airgun signals, as well as their source level estimates, especially when there is significant bathymetric variation over the PoD region such as in the Norwegian Sea and many offshore regions of the world.

#### IV. CONCLUSION

Seismo-acoustic airgun signals have been detected and characterized in the Norwegian Sea at long ranges (175-195 km) from an airgun source system using a large-aperture denselvsampled coherent hydrophone array employing the POAWRS technique. Coherent beamforming of the hydrophone array data is shown to significantly enhance the seismo-acoustic airgun signal SNR and detection range by roughly an order of magnitude over that of a single hydrophone. The detected airgun signals have 10 dB down full bandwidth of 82 Hz, bounded by 22 Hz and 107 Hz at the upper and lower end of this bandwidth. The received pressured levels of the airgun signals are quantified and applied to estimate the backprojected source level distribution. The mean back-projected source level of the airgun source system studied here is found to be 228.8  $\pm$  3.2 dB re 1  $\mu$ Pa at 1 m. The Probability of Detection (PoD) region for these seismo-acoustic airgun signals in the Norwegian Sea are calculated and shown to extend over areas spanning roughly 500 km in diameter, when employing a large-aperture densely-sampled linear coherent hydrophone array as the receiver. This analysis provides an understanding of the horizontal spatial propagation extent of signals from an airgun source system located in the continental shelf region of the Norwegian Sea. This work validates that the POAWRS technique can be extended to monitor seismoacoustic airgun signals from long ranges and in complex ocean environments with highly varying bathymetry. The results of this study can be applied to assess the potential impact of airgun signals on marine organisms.

#### ACKNOWLEDGMENT

This research was supported by the US Office of Naval Research (Ocean Acoustics Program), the Norwegian Institute of Marine Research, Bergen, and the US National Science Foundation.

## REFERENCES

- [1] N. Dutta, "Geopressure prediction using seismic data: Current status and the road ahead," *Geophysics*, vol. 67, no. 6, pp. 2012–2041, 2002.
- [2] R. M. Otis, R. B. Smith, and R. J. Wold, "Geophysical surveys of yellowstone lake, wyoming," *Journal of Geophysical Research*, vol. 82, no. 26, pp. 3705–3717, 1977.
- [3] I. Grevemeyer, C. R. Ranero, E. R. Flueh, D. Kläschen, and J. Bialas, "Passive and active seismological study of bending-related faulting and mantle serpentinization at the middle america trench," *Earth and Planetary Science Letters*, vol. 258, no. 3-4, pp. 528–542, 2007.
- [4] N. Accardo, D. Shillington, J. Gaherty, C. A. Scholz, A. A. Ny-blade, P. Chindandali, G. Kamihanda, T. McCartney, D. Wood, and R. Wambura Ferdinand, "Constraints on rift basin structure and border fault growth in the northern malawi rift from 3-d seismic refraction imaging," *Journal of Geophysical Research: Solid Earth*, vol. 123, no. 11, pp. 10–003, 2018.
- [5] W. S. Holbrook, P. Páramo, S. Pearse, and R. W. Schmitt, "Thermohaline fine structure in an oceanographic front from seismic reflection profiling," *Science*, vol. 301, no. 5634, pp. 821–824, 2003.
- [6] D. Lizarralde, G. J. Axen, H. E. Brown, J. M. Fletcher, A. González-Fernández, A. J. Harding, W. S. Holbrook, G. M. Kent, P. Paramo, F. Sutherland *et al.*, "Variation in styles of rifting in the gulf of california," *Nature*, vol. 448, no. 7152, p. 466, 2007.
- [7] G. Moore, N. Bangs, A. Taira, S. Kuramoto, E. Pangborn, and H. Tobin, "Three-dimensional splay fault geometry and implications for tsunami generation," *Science*, vol. 318, no. 5853, pp. 1128–1131, 2007.
- [8] D. Okaya, T. Stern, S. Holbrook, H. van Avendonk, F. Davey, and S. Henrys, "Imaging a plate boundar using double-sided onshoreoffshore seismic profiling," *The Leading Edge*, vol. 22, no. 3, pp. 256– 260, 2003.
- [9] S. E. Parks, J. L. Miksis-Olds, and S. L. Denes, "Assessing marine ecosystem acoustic diversity across ocean basins," *Ecological Informatics*, vol. 21, pp. 81–88, 2014.
- [10] J. M. Hovem, T. V. Tronstad, H. E. Karlsen, and S. Lokkeborg, "Modeling propagation of seismic airgun sounds and the effects on fish behavior," *IEEE Journal of Oceanic Engineering*, vol. 37, no. 4, pp. 576–588, 2012.
- [11] S. L. Nieukirk, K. M. Stafford, D. K. Mellinger, R. P. Dziak, and C. G. Fox, "Low-frequency whale and seismic airgun sounds recorded in the mid-atlantic ocean," *The Journal of the Acoustical Society of America*, vol. 115, no. 4, pp. 1832–1843, 2004.
- [12] H. Peña, N. O. Handegard, and E. Ona, "Feeding herring schools do not react to seismic air gun surveys," *ICES Journal of Marine Science*, vol. 70, no. 6, pp. 1174–1180, 2013.
- [13] J. C. Goold, "Acoustic assessment of populations of common dolphin delphinus delphis in conjunction with seismic surveying," *Journal of the Marine Biological Association of the United Kingdom*, vol. 76, no. 3, pp. 811–820, 1996.
- [14] S. L. DeRuiter, P. L. Tyack, Y.-T. Lin, A. E. Newhall, J. F. Lynch, and P. J. Miller, "Modeling acoustic propagation of airgun array pulses recorded on tagged sperm whales (physeter macrocephalus)," *The Journal of the Acoustical Society of America*, vol. 120, no. 6, pp. 4100–4114, 2006
- [15] P. Madsen, B. Møhl, B. Nielsen, and M. Wahlberg, "Male sperm whale behaviour during exposures to distant seismic survey pulses," *Aquatic mammals*, vol. 28, no. 3, pp. 231–240, 2002.
- [16] S. Guan, J. Vignola, J. Judge, and D. Turo, "Airgun inter-pulse noise field during a seismic survey in an arctic ultra shallow marine environment," *The Journal of the Acoustical Society of America*, vol. 138, no. 6, pp. 3447–3457, 2015.
- [17] S. L. DeRuiter and K. L. Doukara, "Loggerhead turtles dive in response to airgun sound exposure," *Endangered Species Research*, vol. 16, no. 1, pp. 55–63, 2012.

- [18] D. Wang, H. Garcia, W. Huang, D. D. Tran, A. D. Jain, D. H. Yi, Z. Gong, J. M. Jech, O. R. Godø, N. C. Makris *et al.*, "Vast assembly of vocal marine mammals from diverse species on fish spawning ground," *Nature*, vol. 531, no. 7594, p. 366, 2016.
- [19] H. A. Garcia, C. Zhu, M. E. Schinault, A. I. Kaplan, N. O. Handegard, O. R. Godø, H. Ahonen, N. C. Makris, D. Wang, W. Huang et al., "Temporal–spatial, spectral, and source level distributions of fin whale vocalizations in the norwegian sea observed with a coherent hydrophone array," ICES Journal of Marine Science, vol. 76, no. 1, pp. 268–283, 2018.
- [20] W. Huang, D. Wang, H. Garcia, O. Godø, and P. Ratilal, "Continental shelf-scale passive acoustic detection and characterization of dieselelectric ships using a coherent hydrophone array," *Remote Sensing*, vol. 9, no. 8, p. 772, 2017.
- [21] C. Zhu, H. Garcia, A. Kaplan, M. Schinault, N. Handegard, O. Godø, W. Huang, and P. Ratilal, "Detection, localization and classification of multiple mechanized ocean vessels over continental-shelf scale regions with passive ocean acoustic waveguide remote sensing," *Remote Sensing*, vol. 10, no. 11, p. 1699, 2018.
- [22] Z. Gong, A. D. Jain, D. Tran, D. H. Yi, F. Wu, A. Zorn, P. Ratilal, and N. C. Makris, "Ecosystem scale acoustic sensing reveals humpback whale behavior synchronous with herring spawning processes and reevaluation finds no effect of sonar on humpback song occurrence in the gulf of maine in fall 2006," *PloS one*, vol. 9, no. 10, p. e104733, 2014.
- [23] M. Tolstoy, J. Diebold, L. Doermann, S. Nooner, S. Webb, D. Bohnenstiehl, T. Crone, and R. Holmes, "Broadband calibration of the r/v marcus g. langseth four-string seismic sources," *Geochemistry, Geophysics*, *Geosystems*, vol. 10, no. 8, 2009.
- [24] D. D. Tran, W. Huang, A. C. Bohn, D. Wang, Z. Gong, N. C. Makris, and P. Ratilal, "Using a coherent hydrophone array for observing sperm whale range, classification, and shallow-water dive profiles," *The Journal* of the Acoustical Society of America, vol. 135, no. 6, pp. 3352–3363, 2014.
- [25] W. Huang, D. Wang, and P. Ratilal, "Diel and spatial dependence of humpback song and non-song vocalizations in fish spawning ground," *Remote Sensing*, vol. 8, no. 9, p. 712, 2016.
- [26] C. R. Greene Jr and W. J. Richardson, "Characteristics of marine seismic survey sounds in the beaufort sea," *The Journal of the Acoustical Society* of America, vol. 83, no. 6, pp. 2246–2254, 1988.
- [27] N. C. Makris, O. R. Godø, D. H. Yi, G. J. Macaulay, A. D. Jain, B. Cho, Z. Gong, J. M. Jech, and P. Ratilal, "Instantaneous areal population density of entire atlantic cod and herring spawning groups and group size distribution relative to total spawning population," *Fish and Fisheries*, vol. 20, no. 2, pp. 201–213, 2019.
- [28] J. Northrop and J. Colborn, "Sofar channel axial sound speed and depth in the atlantic ocean," *Journal of Geophysical Research*, vol. 79, no. 36, pp. 5633–5641, 1974.
- [29] C. A. Clark, "Vertical directionality of midfrequency surface noise in downward-refracting environments," *IEEE Journal of Oceanic Engineer*ing, vol. 32, no. 3, pp. 609–619, 2007.
- [30] D. H. Johnson and D. E. Dudgeon, Array signal processing: concepts and techniques. PTR Prentice Hall Englewood Cliffs, 1993.
- [31] M. I. Sezan, "A peak detection algorithm and its application to histogram-based image data reduction," *Computer vision, graphics, and image processing*, vol. 49, no. 1, pp. 36–51, 1990.
- [32] R. J. Urick, "Principles of underwater sound 3rd edition," Peninsula Publising Los Atlos, California, 1983.
- [33] L. E. Kinsler, A. R. Frey, A. B. Coppens, and J. V. Sanders, "Fundamentals of acoustics," Fundamentals of Acoustics, 4th Edition, by Lawrence E. Kinsler, Austin R. Frey, Alan B. Coppens, James V. Sanders, pp. 560. ISBN 0-471-84789-5. Wiley-VCH, December 1999., p. 560, 1999.
- [34] M. D. Collins, "A split-step padé solution for the parabolic equation method," *The Journal of the Acoustical Society of America*, vol. 93, no. 4, pp. 1736–1742, 1993.
- [35] D. Tran, M. Andrews, and P. Ratilal, "Probability distribution for energy of saturated broadband ocean acoustic transmission: Results from gulf of maine 2006 experiment," *The Journal of the Acoustical Society of America*, vol. 132, no. 6, pp. 3659–3672, 2012.
- [36] Z. Gong, M. Andrews, S. Jagannathan, R. Patel, J. M. Jech, N. C. Makris, and P. Ratilal, "Low-frequency target strength and abundance of shoaling atlantic herring (clupea harengus) in the gulf of maine during the ocean acoustic waveguide remote sensing 2006 experiment," *The Journal of the Acoustical Society of America*, vol. 127, no. 1, pp. 104–123, 2010.

- [37] M. Andrews, T. Chen, and P. Ratilal, "Empirical dependence of acoustic transmission scintillation statistics on bandwidth, frequency, and range in new jersey continental shelf," *The Journal of the Acoustical Society of America*, vol. 125, no. 1, pp. 111–124, 2009.
  [38] M. Andrews, Z. Gong, and P. Ratilal, "Effects of multiple scattering, attenuation and dispersion in waveguide sensing of fish," *The Journal of the Acoustical Society of America*, vol. 130, no. 3, pp. 1253–1271, 2011. [37] M. Andrews, T. Chen, and P. Ratilal, "Empirical dependence of acoustic